CLIMA 2016 - proceedings of the 12th REHVA World Congress

volume 6

Heiselberg, Per Kvols

Publication date:
2016

Document Version
Publisher's PDF, also known as Version of record

A New System Sizing for Net Zero Energy Buildings under Uncertainties

Yongjun Sun

Division of Building Science and Technology, City University of Hong Kong, KLN, HK

yongjsun@cityu.edu.hk

Abstract

Net zero energy buildings (NZEBs) have been widely considered to be an effective solution to the increasing energy and environmental problems. Most conventional design methods for NZEB systems are based on deterministic data/information and have not systematically considered the significant uncertainty impacts. Consequently, the conventional design methods lead to popular oversized problems in practice. Meanwhile, NZEB system design methods need to consider customers' actual performance preferences but few existing methods can take account of them. Therefore, this study proposes a multi-criteria system design optimization for NZEBs under uncertainties. In the study, three performance criteria are used to evaluate the overall NZEB system performance based on user-defined weighted factors. Case studies are conducted to demonstrate the effectiveness of the proposed method.

Keywords-net zero energy building; multi-criteria; system sizing; uncertainties; monte carlo simulation

1. Introduction

Buildings consume over 40% of end-use energy worldwide [1] and this percentage for building sector in Hong Kong is even much higher (over 90% of electricity). Such a large part of energy consumption of buildings has imposed significant impacts on the energy conservation and environment protection issues. In order to overcome the energy and environment problems and to pursue sustainable development, net zero energy building (NZEB) has been proposed [2]. NZEB refers to buildings which generate the same amount of energy as they consume over a specific period (e.g. a year). In order to promote the development of NZEBs, many countries/regions have set clear targets for the near future. For instance, U.S. has set a zero energy target for 50% of commercial buildings by 2040 and for all commercial buildings by 2050 [3]. In Europe, the Directive on Energy Performance of Buildings (EPBD) establishes a "nearly net zero energy buildings" as the building target for all new buildings from 2020 [4]. Similarly, the Hong Kong government has set a target for carbon reductions: carbon intensity should be reduced by 50% to 60% by 2020 compared with 2005 baseline [5].

Over the last decades, many NZEB studies have been conducted and they are mainly located in the areas including definitions and performance evaluations of NZEBs [6-7], NZEB and system design [8-9], NZEB integration with renewable energies [10-11], NZEB system control/management optimization [12-13]. Regarding the system design of NZEBs, most conventional methods are based on deterministic data/information and they have not systematically taken account of uncertainty impacts. As a consequence, the conventional design methods can easily cause the problem of oversizing. One simple example is the sizing of air-conditioning system. To select proper size of an air-conditioning system, peak cooling load needs to be properly estimated. It has been shown by many studies that the peak cooling load estimation is associated with uncertainties since building physical parameters cannot be accurately set [14-15] and the weather and the internal load used in the design may be different from the real situation after use [16-18]. In the conventional methods, the peak cooling load is estimated through two simple methods: the worst case scenario method and the safety factor method [19]. In the former method, all the inputs are chosen in such a manner that they will lead to the largest peak cooling load. In the latter method, a safety factor is deliberately added to the peak cooling load that is calculated under typical design condition [20]. Both methods heavily depend on the empirical knowledge of designers. Due to lack of systematic consideration of the uncertainty impacts, oversized design is commonly observed in the applications of these conventional methods [17]. Similar oversized problems are also popular in sizing renewable energy systems. In order to overcome such challenge, the impacts of the uncertainties need to be systematically considered in the system design of NZEBs. With uncertainty distribution identified, statistical method (e.g. Monte Carlo simulation) is one of effective solutions to systematically assess the uncertainty impacts.

Meanwhile, NZEB system design needs to consider customers' different performance preferences, but unfortunately few existing methods can take account of them. It is very likely that different customers may have different performance preferences. In other words, multiple pre-defined performance indices (e.g. initial cost, indoor thermal comfort and building-grid interactions) in the NZEB system design are not equally important to customers. For instance, some customers may consider the initial system cost is more important than other performance indices; but other customers may consider the opposite. In this case, the multi-criteria decision making (MCDM) is needed for the NZEB system design optimization. MCDM is an effective technique to evaluate the overall performance of each alternative and identify the optimal one by assessing the potential costs, benefits and risks [21]. This technique has already been applied in building system design [22-24]. Balcomb adopted the MCDM method to compare several building design alternatives including insulation, glazing, duct leakage, thermal mass etc. [23]. Considering uncertainty impacts, Sten compared two different design strategies whether adding cooling system or not in thermal zone and made a choice with Bayesian decision theory [24]. Hopfe applied analytic hierarchy process to compare the performance of two buildings in terms of initial cost, architectural form and symbolism etc. [16]. NZEB system sizing is actually important for minimizing the initial system cost, ensuring good indoor thermal comfort and minimizing the grid stress caused by the power mismatch. Power mismatch (i.e. difference between building power generation and demand) is an inherent problem to NZEBs. The renewable energy generation is of high

uncertainty and intermittent nature. The power generated is not only discontinuous but also fluctuate, which causes the fluctuations of real time power mismatch. Connection to bulk grid is a popular approach to solve the power mismatch problem in NZEBs. One major limitation of the approach is the direct import/export of fluctuating power from/to the grid can easily result in stresses on the grid power balance and the power supply quality. Such stress can be described by the grid interaction index [25]. When cost, indoor thermal comfort and grid stress are considered simultaneously, the NZEB system design becomes a problem of MCDM.

This paper, therefore, proposes a multi-criteria system design optimization for NZEBs under uncertainties. The proposed method is constituted of three parts. The first part is to identify the peak cooling load uncertainty distribution using Monte Carlo simulation with three types of building parameter uncertainties considered. The second part is to size the air-conditioning system and the renewable system (including PV panel and wind turbine) according to the identified peak load distribution. The third part is to select the optimal system size based on the overall performance evaluation results in terms of the pre-defined criteria. Case studies are also conducted to demonstrate the effectiveness of the proposed method through comparison with one conventional system design method.

2. Methodology

2.1 Overview of the multi-criteria system design optimization method

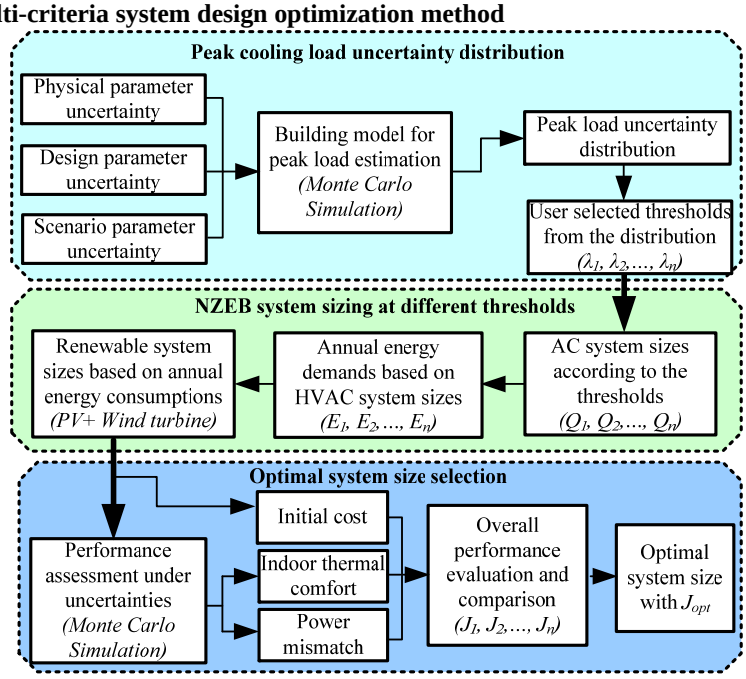

Figure-1 Multi-criteria system design optimization for NZEBs under uncertainties

Figure-1 shows the basic idea of the multi-criteria system design optimization method for NZEBs under uncertainties. In this study, the performance criteria concerning system initial cost, indoor thermal comfort and grid stress caused by power mismatch are considered. The proposed method consists of three parts. In the first part, the uncertainty of the peak cooling load is identified using the stochastic inputs and the Monte Carlo simulation. Peak cooling load uncertainty is caused by the uncertainties of physical parameter, design parameter and scenario parameter which can be described using statistic distributions [26]. Monte Carlo method is a sample-based method which relies on repeated random sampling to obtain numerical results. Due to its simplicity and convenience, Monte Carlo method has been widely used to obtain model output distribution especially in the presence of multiple input uncertainties [27].

In the second part, both the air-conditioning system size and the renewable system size are determined according to the thresholds (i.e. λ_1, λ_2, …, λ_n) selected from the identified peak load distribution. Different thresholds represent different potential risks that the corresponding air-conditioning capacity (i.e.Q_1, Q_2,…,Q_n) cannot fulfill the estimated peak cooling load. Such potential risks can be evaluated using the cumulative probability of the obtained peak load uncertainty. A smaller threshold implies a larger potential risk. Based on the determined air-conditioning system sizes, the associated building annual energy demands (i.e. E_1, E_2,…,E_n) are estimated. Due to the goal of net zero energy in a NZEB, these estimated annual energy demands are used to determine the sizes of the renewable system.

In the third part, the optimal sizes of the air-conditioning system and the renewable system are selected according to the overall performance evaluation results. In order to optimize the system sizes under the established multi-criteria, performance trade-offs caused by the system size changes need to be considered. For instance, a larger air-conditioning system size can provide a better indoor thermal comfort but will cause a more expensive initial cost. Meanwhile, the uncertainty impacts is systematically investigated and evaluated through Monte Carlo simulation in terms of initial cost, indoor thermal comfort and grid stress. According to the weighted factors assigned by users to different performance criteria,

the overall performance scores (J_1, J_2,…, J_2) are obtained and compared at different thresholds. The system sizes with the highest overall performance score are selected as the optimal ones.

2.2 Peak cooling load uncertainty identification

Cooling load uncertainty is mainly caused by three types of parameter uncertainties: physical parameter uncertainty, design parameter uncertainty and scenario parameter uncertainty [28]. Physical parameter refers to physical properties of materials and they are mostly identified as the standard input parameters in conventional design methods and not influenced by designers. Design parameter refers to pre-set working condition of building during the planning process and they are fully determined by the decision maker/ designers. Scenario parameter refers to parameters that are related to the real-time operation of the building during its life time. They are not measurable and hard to control [29]. Studies have shown that all these parameters are associated with uncertainties which have significant impacts on building system design [17, 28-29]. The characteristics of these uncertainties can be described by statistical distributions (e.g. normal distribution, triangular distribution) [26]. In this study, the input parameters and their uncertainty distributions used are as shown in Table-1.

Table-1 Building parameter uncertainty distributions

Types	Parameters	Distributions	Reference
Physical parameters	U value of window	Normal distribution	[14-15]
	Internal shading coefficient	Normal distribution	
	External shading coefficient	Normal distribution	
	Internal conductive heat transfer rate	Normal distribution	
	External conductive heat transfer rate	Triangular distribution	
Design parameters	Occupant number	Normal distribution	[26]
	Computer number	Normal distribution	
	Light ratio	Normal distribution	
	Inflation	Normal distribution	
	Ventilation	Normal distribution	
Scenario parameters	Ambient temperature	Normal distribution	[16-18]
	Ambient relative humidity (RH)	Normal distribution	

These parameter uncertainties are taken as the inputs of a constructed virtual building. For each uncertain parameter, a row of 100,000 samples is generated from the assigned distribution using random sampling approach. An input matrix is formed by all these 12 rows of samples and the input matrix is sent to the constructed building for Monte Carlo simulation. After the Monte Carlo simulation, the associated 100,000 peak loads are obtained for its uncertainty distribution identification.

2.3 Net zero energy building system sizing

Multiple thresholds are selected by user from the identified peak load distribution. Each threshold determines its corresponding air-conditioning system size. In other words, the air-conditioning system size needs to meet the user selected threshold, as shown by (1).

$$Q_i = \lambda_i \quad i = 1, 2..., \mathrm{n} \tag{1}$$

where, Q is the cooling capacity of the air-conditioning system; λ is the user selected threshold; n is the number of the thresholds.

After the air-conditioning system size Q is determined, the power consumption of air-conditioning system at any cooling load CL can be estimated, as shown in (2). With the power consumptions of the air-conditioning system and the lighting system known, the associated building annual energy demand can be calculated as (3).

$$Pow_{AC} = f(\mathrm{Q}, \mathrm{CL}) \tag{2}$$

$$E_{dem} = \sum (\mathrm{Pow}_{AC} + \mathrm{Pow}_{light}) \times \Delta t \tag{3}$$

where, E_{dem} is the building annual energy demand; Pow is the power consumption; CL is the cooling load; Δt is the time interval and subscripts AC and $light$ represent the air-conditioning system and the lighting system.

With the estimated building annual energy demand E_{dem}, the size of the renewable system can be determined. In this study, two types of renewable systems (i.e. PV panel and wind turbine) are used. The sum of their energy supplies needs to meet the building annual energy demand, as shown in (4).

$$\begin{aligned} E_{PV,\mathrm{sup}} &= \varphi E_{dem} \propto A \\ E_{Wind,\mathrm{sup}} &= (1-\varphi) E_{dem} \propto Num \end{aligned} \tag{4}$$

where, $E_{PV,sup}$ and $E_{Wind,sup}$ represent the energy supplies from the PV panel and the wind turbines; coefficient φ is the percentage of the overall energy supply from the PV system; A and Num are the PV panel area and the number of the wind turbines.

2.4 Optimal system size selection

The multi-criteria function is established as (5). It consists of three performance scores, i.e. initial cost score Γ_{cost}, thermal comfort score $\Gamma_{\mathrm{comfort}}$ and grid stress score Γ_{stress}. The performance score Γ is quantified using the linear

interpolation between the least preferred performance P_{least} and the most preferred performance P_{most}, as expressed in (6). For one performance criterion, the most preferred performance is assigned the score of 100, and the least preferred option is assigned the score of 0.

$$J = \alpha_{cost} \times \Gamma_{cost} + \alpha_{comfort} \times \Gamma_{comfort} + (1 - \alpha_{cost} - \alpha_{comfort}) \times \Gamma_{grid} \tag{5}$$

$$\Gamma = \frac{P - P_{least}}{P_{most} - P_{least}} \times 100 \tag{6}$$

where, α_{cost} *and* $\alpha_{comfort}$ are the weighted factors assigned by users according to their actual preference; Γ represents the performance score; and the subscripts *cost, comfort* and *stress* are system initial cost, thermal comfort and grid stress.

The initial cost is determined by the air-conditioning system size and renewable system size. It is calculated by (7). Regarding the air-conditioning system, the initial cost is also calculated using linear interpolation on the prices of products. With regard to the renewable system, the initial cost of PV panel is the product of the area and unit price; the initial cost of wind turbine is the product of number and the price of single wind turbine.

$$P_{cost} = \beta_1 \times \frac{Q}{Q_{baseline}} + \beta_2 \times A + \beta_3 \times Num \tag{7}$$

where, β_1 is the price of air-conditioning system with capacity $Q_{baseline}$; β_2 is the unit price of PV panel and β_3 is the price of one wind turbine.

The thermal comfort is evaluated using the total failure time in which the cooling supplied from the air-conditioning system CL_{sup} cannot meet the actual cooling load CL_{act}, as expressed by (8). A larger failure time indicates the worse indoor thermal comfort.

$$P_{\text{comfort}} = \sum \Delta t_i \ (\text{CL}_{\text{sup,i}} < \text{CL}_{act,i}) \tag{8}$$

The average grid stress caused by the power mismatch can be depicted using the grid interaction index [25], as shown by (9). The index represents fluctuations of energy exchanges of building with grid. The smaller the index, the smaller the grid stress.

$$P_{mismatch} = STD\left(\frac{Pow_{\text{mis},i}}{\max\left[|\ \text{Pow}_{\text{mis,1}}\ |, |\ \text{Pow}_{\text{mis,2}}\ |, \ldots, |\ \text{Pow}_{\text{mis,8760}}\ |\right]}\right) \tag{9}$$

where, STD is the standard deviation; Pow_{mis} is the power mismatch between the building power supply and building power demand; subscript *i* represents i^{th} hour.

3. Simulation Study Platform

3.1 Building description

With its powerful transient simulation capability, TRNSY [30] was used in this study to simulate a case building and its air-conditioning and renewable systems. The building is a low-rise academic building with 10 identical floors and 30m high in total. Each floor has two same sized classrooms. The dimensions of the classroom are 7.6m×6m with the capacity of 16 occupants. Each classroom has one window facing to the west with the size of 4m×1.5m. The indoor temperature was set to 25 ℃, and the relative humidity was set to 50%. The ventilation rate was set to be 10 ACH and 5 ACH in the occupied hours (6:00 am to 22:00 pm) and the unoccupied hours respectively. The infiltration rate was set to be 0.2 ACH. There were 16 computers with a nominal power of 140W in each classroom. The computers were switched on in the occupied hours and off in the other time. The power density of the lighting system (i.e. eight Halogen lights) in each classroom was 55W/m^2. The parameter uncertainties used in the study for peak load estimation are as shown in Table-2.

Table-2 Building parameter uncertainties used for peak load estimation

No.	Parameters	Base value	Distribution	Truncation	Rounding
1	Occupant number	16	$N(16, 2^2)$	[12, 20]	Yes
2	Computer number	16	$N(16, 3^2)$	[12, 16]	Yes
3	Light ratio	1	$N(1, 0.2^2)$	[0.5, 1]	No
4	Inflation (ACH)	0.2	$N(0.2, 0.05^2)$	[0.15, 0.35]	No
5	Ventilation (ACH)	10	$N(10, 0.5^2)$	[8.5, 11.5]	No
6	U value of window $(kJ/(hr \cdot m^2K))$	8.17	$N(8.17, 0.4^2)$	[7, 9.5]	No
7	Internal shading coefficient	0.5	$N(0.5, 0.1^2)$	[0.3, 0.7]	No
8	External shading coefficient	0.2	$N(0.2, 0.05^2)$	[0.05, 0.2]	No
9	Internal convection transfer rate $(kJ/(hr \cdot m^2K))$	11	$N(11, 0.5^2)$	[9.5, 15]	No
10	External convection transfer rate $(kJ/(hr \cdot m^2K))$	68.4	T(43.2,68.4, 82.8)	—	No
11	Ambient temperature (℃)	33.56	$N(33.56, 1.5^2)$	[32, 34]	No
12	Ambient relative humidity (%)	55	$N(5.5, 2.5^2)$	[50, 60]	No

3.2 Air-conditioning system description

The air-conditioning system is as shown in Figure-2. In the chiller plant, constant speed pumps were used in the primary (i.e. chilled water production) side; while variable speed pumps were used in the secondary (i.e. chilled water distribution) side. The set-point for the supply chilled water was 7℃ and for the supply air temperature of the air-handling unit (AHU) was 16℃, which was controlled by adjusting the speed of the pumps in the secondary loop. The condenser water loop mainly consisted of a constant speed pump, a cooling tower equipped with a variable speed fan. The outlet water temperature of cooling tower was set to be 5℃ above the wet-bulb temperature of ambient air. Such temperature difference was maintained through adjusting the peed of the fan in the cooling tower [15].

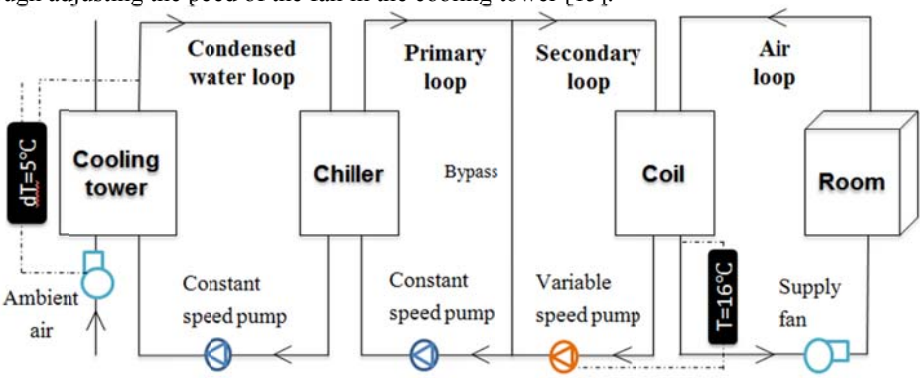

Figure-2 Schematics of the air-conditioning system

The main steps for the component sizing and component power estimations of the air-conditioning system are illustrated as follows. The chiller plant was sized to have a rated cooling capacity which can meet the chosen peak load (i.e. the threshold). The power consumption of the chiller W_c was calculated according to the nominal COP, its actual supplied cooling Q_c, and the fraction of full load power-*FFLP* [30].

$$W_c = 3600 \times FFLP \times Q_c / COP_{nom} \tag{10}$$

3.3 Renewable system description

Both PV panels and wind turbines were used in the study for energy supply. Type 562 from TRNSYS was used to simulate the power supply of the PV panel system. 11 represents the relation between the PV panel power output and the solar radiation. Type 90, i.e. wind energy conversion system (WECS), was chosen in the study to simulate the power supply of the wind turbines. 12 represents the relation between the wind turbine power output and the wind velocity.

$$P_{pv} = (\tau\alpha)_n (IAM) I_T \eta A \tag{11}$$

where, $(\tau\alpha)_n$ is the transmittance-absorptance product of the PV cover for solar radiation at a normal angle of incidence, ranging from 0 to 1; *IAM* is the combined incidence angle modifier for the PV cover material, ranging from 0 to 1 and it can be calculated using the entered information about the cover material's refractive index, thickness, thermal conductivity, and extinction coefficient; I_T is the total amount of solar radiation incident on the PV collector surface (kJ/hr.m^2); η is the overall efficiency of the PV array; and A is the PV surface area (m^2).

$$P = C_p \rho A_R U_0^3 \tag{12}$$

where, *P* is power output (kW); ρ is air density (kg/m^3); A_R is rotor area (m^2); U_0 is wind velocity in the free stream (m/s); power coefficient C_p is a function of the axial induction factor.

4. Case Studies

4.1 Peak load uncertainty identification

Random sampling approach was used to generate 100,000 samples for each uncertain parameter listed in Tabl-2. The samples were used in the Monte-Carlo simulation to investigate the characteristics of the peak cooling load. The generated 100,000 peak cooling loads were put into a histogram and its distribution is as shown in Figure-3. The horizontal axis displays the range of the peak cooling load uncertainty. The left vertical axis is the frequency that a particular level of peak cooling load occurs, and the right one is the cumulative probability of the peak cooling load. The figure shows that the peak cooling load uncertainty can be approximately described by a normal distribution. The mean value of the normal distribution μ was 193kW, and the standard deviation σ was about 6kW.

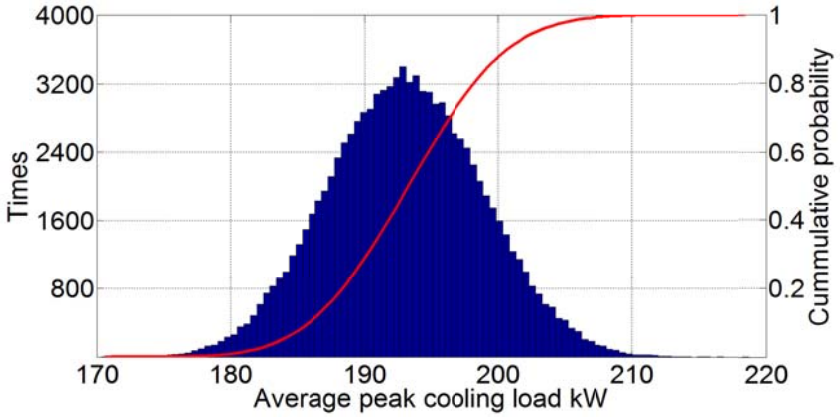

Figure-3 Histogram of the identified peak cooling load uncertainty

Based on the obtained peak cooling load uncertainty, seven different thresholds (λ_1, λ_2, λ_3, λ_4, λ_5, λ_6, λ_7) were selected for sizing the air-conditioning system, as shown in Tabl-3. Each threshold had its own potential risk that the corresponding capacity cannot fulfil the estimated peak cooling load. For example, if the λ was chosen to be 209.65 kW (i.e. $\lambda=\mu+3\sigma$), the potential risk was only 0.15% (i.e. 1-the cumulative probability) that the selected cooling capacity cannot fulfil the estimated peak load. In other words, 99.85% of the estimated peak load uncertainty can be satisfied by the corresponding air-conditioning size with capacity of 209.65 kW.

Table-3 Seven thresholds and their potential risks

λ	Cumulative probability density	Risk	Cooling Capacity (kW)
$\lambda_1=\mu$	50.00%	50.00%	Q_1=192.97
$\lambda_2=\mu+0.5\sigma$	69.15%	30.85%	Q_2=195.91
$\lambda_3=\mu+\sigma$	84.15%	15.85%	Q_3=198.82
$\lambda_4=\mu+1.5\sigma$	93.32%	6.68%	Q_4=201.68
$\lambda_5=\mu+2\sigma$	97.70%	2.30%	Q_5=204.51
$\lambda_6=\mu+2.5\sigma$	99.38%	0.62%	Q_6=207.20
$\lambda_7=\mu+3\sigma$	99.85%	0.15%	Q_7=209.65

4.2 Building system sizing according to selected thresholds

In the study, the size of the air-conditioning system was chosen according to the selected thresholds. According to (1), seven different sizes of the air-conditioning system were chosen correspondingly. Different sizes of the air-conditioning system had different annual energy consumptions, as shown in Table-4. The maximum PV panel area and the maximum number of the wind turbine with the rated power of 9 kW are also as shown in the table. The maximum PV panel area/the maximum number of wind turbine meant the associated annual energy demand can be supplied by the PV system/the wind turbine alone. Based on the price information of the systems, the initial cost can be calculated for the air-conditioning system and the renewable systems. Compared with the energy consumptions of the other systems (e.g. lighting system, lift system), the annual energy of the air-conditioning system was much larger and also much more complex to estimate. Hence, in the study, the air-conditioning system energy consumption was considered for the sizing of the renewable systems. In practice, the other system energy consumptions can be simply added for the renewable system sizing.

Table-4 Air conditioning system annual energy consumption and corresponding renewable system sizes

No	Air-conditioning size (kW)	Annual energy consumption (10^5kWh)	Maximum PV panel area (10^3m^2)	Maximum Wind turbine number
1	Q_1=192.97	3.3222	2.1868	28
2	Q_2=195.91	3.3871	2.2295	29
3	Q_3=198.82	3.4257	2.2549	29
4	Q_4=201.68	3.4609	2.2781	29
5	Q_5=204.51	3.4979	2.3024	30
6	Q_6=207.20	3.5319	2.3248	30
7	Q_7=209.65	3.5650	2.3466	30

With different values of φ selected in (4), the resulting power mismatches had different characteristics in magnitudes and fluctuations. Power mismatches with different characteristics resulted in different grid interaction indices representing the grid stress caused by the fluctuating energy exchange between the building and the grid. In this study, the φ values (representing the percentages of the overall energy supplied by the PV panel system) were changed from 0 to 1 with the step length of 0.1. Hence, for each sized air-conditioning system, there were 11 different size combinations of the PV panel and

the wind turbine. With a set of given weighted factors, the size combination with the highest performance score was selected as the renewable system.

4.3 Performance evaluation and system size optimization

In the proposed method, a set of weighted factors need to be defined before the overall performance evaluation expressed by (5). In the study, the values of the weighted factors were assigned as α_{cost}=0.3 and $\alpha_{comfort}$=0.4. In order to consider the uncertainty impacts, the Monte Carlo simulation of 80 years was conducted for the performance assessment. The building parameter uncertainties in Table-2 were sampled and used in the performance assessment. Considering the impacts of the scenario parameters on the power generation of the renewable systems, a normal distribution (i.e. N~(0, 10%)) was added to describe the uncertainties of solar radiation and wind speed [33]. The unit price of PV panel and the wind turbine with the rated power of 9 kW were 16 HKD/m^2 and 57,000 HKD respectively [34-35]. The associated initial costs of the seven different sized air-conditioning system were selected as 2,083,080 HKD, 2,109,710 HKD, 2,136,400 HKD, 2,162,210 HKD, 2,188,190HKD, 2,212,420HKD and 2,235,140 HKD with reference to [29]. Note that the mean values of the Monte Carlo simulation results were used for the performance score calculations.

In this study, the indoor thermal comfort was evaluated using the total failure time in which the cooling supplied cannot meet the actual cooling load demand as expressed by (8). Since the failure time was only dependent on the air conditioning system size, the thermal comfort evaluations did not need to consider the renewable system sizes. Figure-4 (a) shows the mean failure time of the seven air-conditioning system sizes selected in Section 4.2. It can be observed that the failure time decreased with the size/capacity increase of the air-conditioning system. More importantly, the reduction of the failure time followed an exponential way instead of a linear way. The exponential reduction indicated that the indoor thermal comfort deterioration rates were different at different system sizes. For instance, the failure time rapidly increased by 3.64 hour as the size reduced from 195.91 kW to192.97 kW; while it only increased by 0.44 hour as the size reduced from 209.65 kW to 207.2 kW. Such comfort deterioration rate difference need to be well considered for the sizing of air-conditioning system especially as multiple criteria are considered. Otherwise, undesirable results will be expected. For instance, the size increase of a system with enough capacity can only contribute little to the reduction of the failure time (i.e. the improvement of the indoor thermal comfort) but cause significant initial cost increase. The associated performance scores calculated using (6) is shown in Figure-4 (b). The least preferred performance for the score calculation was the largest failure time occurring in the Monte Carlo simulation, i.e. 20 hours; while the most preferred performance for the score calculation was the smallest failure time occurring in the Monte Carlo simulation, i.e. 0 hour. Basically, a larger failure time resulted in a lower performance score.

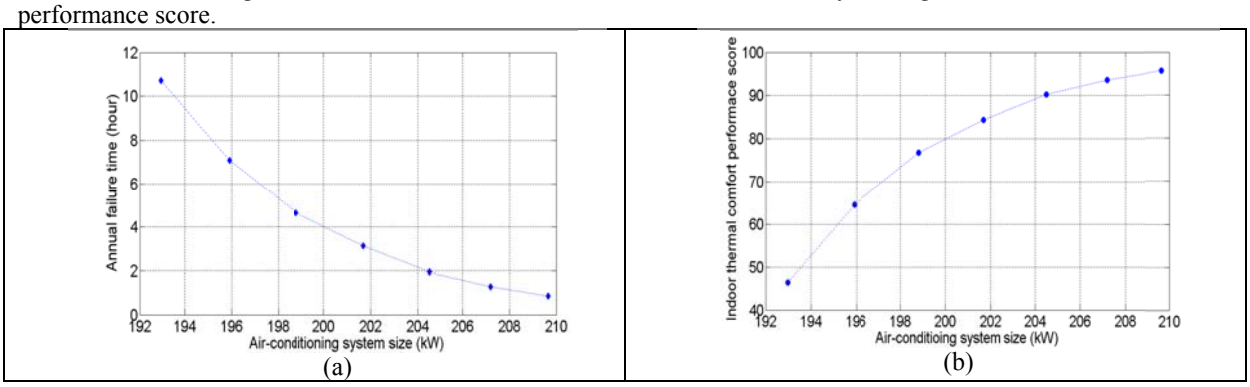

(a) (b)

Figure-4 Mean failure time (a) and thermal comfort performance score (b) variations with air-conditioning system sizes

The fluctuations of power mismatch can cause the stress on grid power balance and power supply quality. The grid stress can be described using the grid interaction index as expressed by (9). The grid interaction index was mainly dependent on the size combination of the renewable energy system. Figure-5 (a) shows the interaction index at different size combinations. The renewable system size combination was determined by parameter φ which represents the percentage of overall building energy supplied by PV system. The associated performance score is shown in Figure-5 (b). The least preferred performance for the score calculation was the largest grid interaction index occurring in the Monte Carlo simulation, i.e. about 0.22; while the most preferred performance for the score calculation was the smallest grid interaction index occurring in the Monte Carlo simulation, i.e. about 0.16. From Figure-5, it can be observed that single type of renewable system (either 100% PV system or 100% wind turbine) had the largest grid interaction indices that represented the largest power mismatch fluctuations and correspondingly the largest grid stress. The best size combination was when PV system provided about 50 percent of the building overall energy demand. Compared with the pure PV system (i.e. 100% PV), the best renewable system size combination (i.e. 50% PV) significantly reduced the fluctuations of the power mismatch as shown in Figure-6.

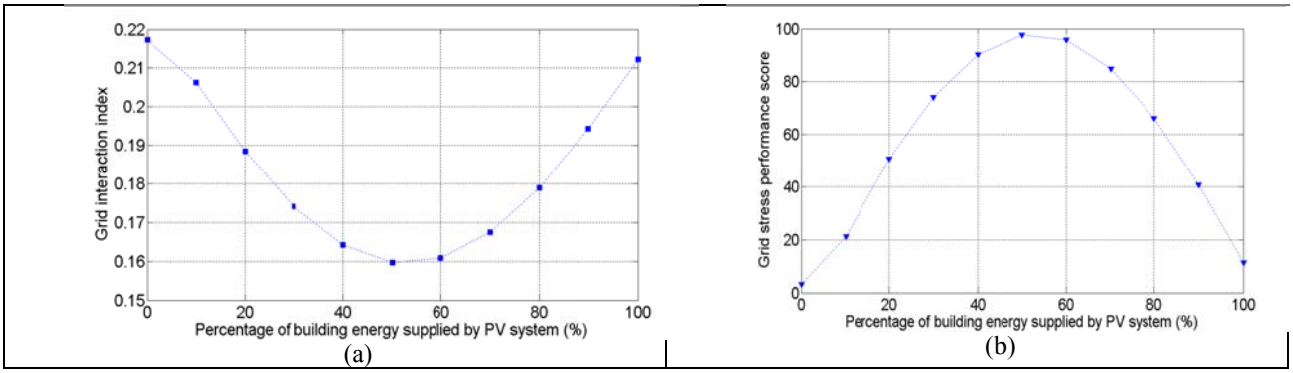

Figure-5 Mean grid interaction index (a) and grid stress performance score (b) variations with PV system sizes

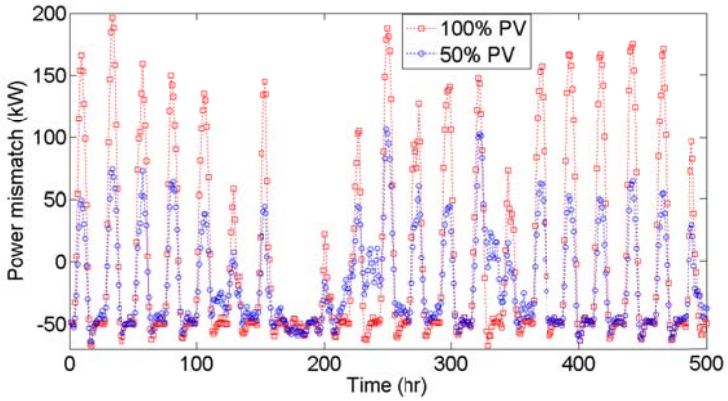

Figure-6 Power mismatches comparison between two renewable system size combinations

Given the weighted factors and the price information of the systems, the overall performance scores calculated by (5) are shown in Figure-7. It can be clearly observed that both the air-conditioning system size and the renewable system size combination played significant roles in the multi-criteria system optimization of a NZEB. The overall performance score varied in a wide range between 34 and 78. Based on the highest overall performance score (i.e. 78), the associated optimal system sizes can be determined. In the study, the optimal air-conditioning system size was 201.68 kW. The optimal PV panel area was 1139 m^2 and the wind turbine number was 15. Such a wide range variation of the overall performance score also demonstrated the air-conditioning system size and the renewable system size combination needed to be carefully selected. Otherwise, the design building systems in a NZEB can have a very poor overall performance. Relatively high scores can be obtained at the PV system providing building energy percentages around 50%. The main reason was that the grid stress representing by the grid interaction index was significantly reduced when about 50% of building energy was supplied by the PV system, as shown in Figure-5. With the air-conditioning system size increase, the overall performance firstly increased to a peak value and then reduced. The main reason was the performance tradeoff between the indoor thermal comfort and the initial cost. In the air-conditioning system size increase process, the initial cost increased (i.e. the initial cost performance score reduced) at a relatively constant rate. However, in the air-conditioning system size increase process, the failure time decreased (i.e. the indoor thermal comfort score increased) at different rates (i.e. an exponential rate), as shown in Figure-4. The thermal comfort performance score was significantly improved as the air-conditioning system size was increased from a small capacity. In this case, the overall performance score increased due to that the performance score increase of the thermal comfort was larger than the associated performance score reduction of the initial cost. The further increase of the air-conditioning system size with a large capacity can only contribute little to the reduction of the failure time and the improvement of the indoor thermal comfort, as shown in Figure-4. In this case, the overall performance score decreased due to that the performance score increase of the thermal comfort was smaller than the performance score reduction of the initial cost. It should be mentioned that the final optimal system sizes from the proposed method depends on the user defined weighted factors according to their actual preferences. In other words, as different weighted factors selected, different optimal system sizes will be correspondingly obtained using the proposed multi-criteria NZEB system optimization method.

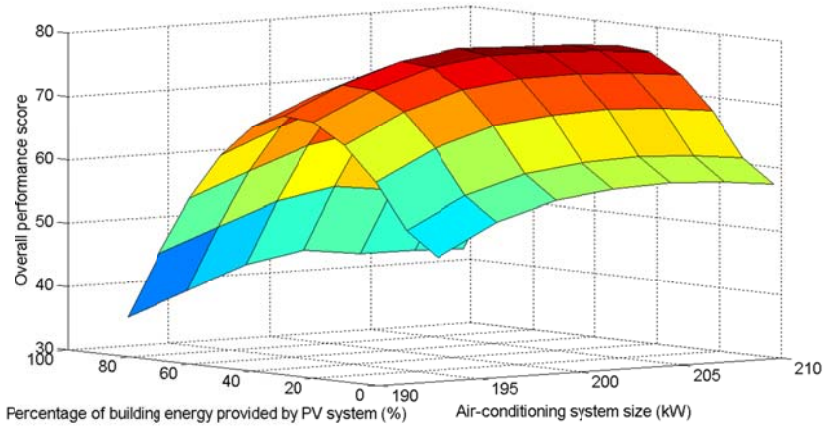

Figure-7 Overall performance score variations with NZEB system sizes

5 Conclusions

The study proposes a multi-criteria system design optimization for NZEBs under uncertainties. The study results show that the peak cooling load uncertainty approximately follows a normal distribution and it needs to be well considered for the sizing of the air-conditioning system as multiple criteria considered. With the size decrease of the air-conditioning system, the indoor thermal comfort representing by the failure time deteriorated in an exponential way. It is also found that the renewable system size combination plays an important role in the grid stress caused by the power mismatch. With the given weighted factors and the price information, the overall performance varies in a large range (i.e. from 34 to 78) as the building system sizes change. The study results demonstrate that the proposed method can effectively identify the optimal building system sizes based on the obtained overall performance scores.

This method provides an effective way to help designers systematically investigate the uncertainty impacts of building parameters on NZEB system performance in terms of multiple criteria. Meanwhile, in the NZEB system design optimization, the proposed method can provide flexibility to the users in selecting different weighted factors to each criterion according to their actual performance preferences/requirements.

Acknowledgement

The research work presented in this paper is financially supported by the Start-up grant of City University of Hong Kong (No. 7200398).

References

[1]. ASHRAE, ASHRAE handbook-HVAC applications (SI), ASHRAE Inc., Atlanta, USA, 2011.
[2]. I. Visa, M.D. Moldovan, M. Comsit, A. Duta, Improving the renewable energy mix in a building toward the nearly zero energy status, Energy and Buildings 68 (2014) 72-78.
[3]. D. Crawley, S. Pless, P. Torcellini, Getting to net zero, ASHRAE Journal 51 (2009) 18–25.
[4]. Directive 2010/31/EU of the European Parliament and of the Council of 19 May 2010 on the energy performance of buildings, Official Journal of the European Union, Legislation 153, (2010) 13–35.
[5]. G. Li. Achieving Zero Carbon for Buildings in a Densely Populated City and a Subtropical Climate, Urban Density & Sustainability, Sustainable Building 2013 Hong Kong Regional Conference.
[6]. A.J. Marszal, P. Heiselberg, J.S. Bourrelle, Zero Energy Building – A review of definitions and calculation methodologies, Energy and Buildings 43 (2011) 971-979.
[7]. P. Torcellini, S. Pless, M. Deru, D. Crawley, Zero Energy Buildings: A Critical Look at the Definition, in: ACEEE Summer Stud, Pacific Grove, California, USA, 2006.
[8]. C.J. Kibert, Net-zero energy buildings: designing to nature's budget. Conference in central Europe towards sustainable building, Prague, 2010.
[9]. A. Robert, M. Kummert, Designing net-zero energy buildings for the future climate, not for the past, Building and environment 55 (2012) 150-158
[10]. W. Zeiler, G. Boxem, Net-zero energy building schools, Renewable Energy XXX (2012) 1-5.
[11]. L.P. Wang, J. Gwilliam, P. Jones, Case study of zero energy house design in UK, Energy and Building 41 (2009) 1215-1222.
[12]. D. Kolokotsa, D. Rovas, E. Kosmatopoulos, K. Kalaitzakis, A roadmap towards intelligent net zero- and positive-energy buildings, Solar Energy 85 (2011) 3067-3084
[13]. S. Cho, J.S. Lee, C.Y. Jang, ect. 2008. Development of Integrated Operation, Low-End Energy Building Engineering Technology in Korea. EKC2008 Proceedings of the EU-KOREA conference on science and technology, Springer Proceedings in Physics, 2008.
[14]. F. Domínguez-Muñoz, B. Anderson, J.M. Cejudo-López, A. Carrillo-Andrés, Uncertainty in the thermal conductivity of insulation materials, Energy and buildings 42 (2010) 2159-2168.
[15]. ASHRAE. ASHRAE Handbook–Fundamentals, ASHRAE Inc., Atlanta, USA, 2009.
[16]. C.J. Hopfe, J.L.M. Hensen, Uncertainty analysis in building performance simulation for design support, Energy and Buildings 43 (2011) 2798–2805
[17]. E. Djunaedy, K. Wymelenberg, B. Acker, H. Thimmana, Oversizing of HVAC system: Signatures and penalties, Energy and Buildings 43 (2011) 468-475.
[18]. K.J. Lomas, H. Eppei, Sensitivity analysis techniques for building thermal simulation programs, Energy and buildings 19 (1992) 21-44.
[19]. S.K. Wang, Handbook of air conditioning and refrigeration, 2nd Edition, McGraw-Hill, Two Penn Plaza, New York, USA, 2000.
[20]. A.A. Bell, HVAC Equations, Data, and Rules of Thumb, 2nd Edition, McGraw-Hill, Two Penn Plaza, New York, USA, 2007.
[21]. J.S. Dodgson, M. Spackman, A. Pearman, L.D. Phillips, Multi-criteria analysis: a manual, Department for Communities and Local Government, London, 2009.
[22]. J.P. Huang, K.L. Poh, B.W. Ang, Decision analysis in energy and environmental modeling, Energy 20 (1995) 843-855.
[23]. J.D. Balcomb, A. Curtner, Multi-criteria decision-making process for buildings, 35th Intersociety of Energy Conversion Engineering Conference and Exhibit (IECEC), Las Vegas, USA, 2000.

[24]. S. De Wit, G. Augenbroe, Analysis of uncertainty in building design evaluations and its implications, Energy and Buildings 34 (2002) 951-958.
[25]. J. Salom, J. Widen, J. Candanedo, I. Sartori, K. Voss, A. Marszal, Understanding net zero energy building: Evaluation of load matching and grid interaction indicators, Proceedings of Building Simulation: 12th Conference of International Building Performance Simulation Association, Sydney, 2011.
[26]. I.A. Macdonald, Quantifying the effects of uncertainty in building simulation, University of Strathclyde, 2002.
[27]. F. Domínguez-Muñoz, J.M. Cejudo-López, A. Carrillo-Andrés, Uncertainty in peak cooling load calculations, Energy and Buildings 42 (2010) 1010-1018.
[28]. C.J. Hopfe, Uncertainty and sensitivity analysis in building performance simulation for decision support and design optimization, Eindhoven Uni. of Technology, Eindhoven, Netherlands, 2009.
[29]. P. Huang, G.S. Huang, Y. Wang, HVAC System Design under Peak Load Prediction Uncertainty Using Multiple-Criterion Decision Making Technique, Energy and Buildings, (2015) In Press.
[30]. S.A. Klein, TRNSYS 16 Program Manual, Solar Energy Laboratory, University of Wisconsin-Madison, Madison, USA, 2007.
[31]. ASHRAE Handbook, HVAC Systems and Equipment, American Society of Heating, Refrigerating, and Air Conditioning Engineers, Atlanta, GA, 1996.
[32]. W.T. Grondzik, Air-conditioning system design manual, 2nd Edition, ASHRAE Inc., Atlanta, USA, 2007.
[33]. D.R. Myers, Solar radiation modeling and measurements for renewable energy applications: data and model quality, Energy 30 (2005) 1517–1531
[34]. D. Feldman, G. Barbose, R. Margolis1, R. Wiser, N. Darghouth, and A. Goodrich, Photovoltaic (PV) Pricing Trends: Historical, Recent, and Near-Term Projections, U.S. Department of Energy, 2012
[35]. E. Lantz, R. Wiser, M. Hand, IEA Wind Task 26: The Past and Future Cost of Wind Energy, National Renewable Energy Laboratory, USA, 2012